Final Report for NASA Grant NAG-1-2084 submitted to

THE NATIONAL AERONAUTICS AND SPACE
ADMINISTRATION

DETERMINATION OF SPECTRAL LINE PARAMETERS IN SELECTED PORTIONS OF THE INFRARED SPECTRUM OF WATER VAPOR

by

Karen Keppler Albert
Frohalpstrasse 19
CH-8038 Zürich, Switzerland

Formerly of
Department of Physics
Getty College of the Arts and Sciences
Ohio Northern University
Ada, OH 45810

Dr. Karen Keppler Albert
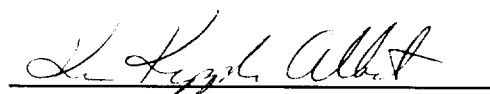Phone: (41) - 1- 481- 2562
Email: kkalbert@bluewin.ch

TABLE OF CONTENTS

I. Executive summary

Pressure broadening and pressure-induced shift coefficients due to water and nitrogen have been determined for water vapor transitions in the CO_2 region of interest to Project HALOE. The temperature dependences of the widths and shifts have also been determined for selected transitions in this region. Results have been compared with values available in the literature. The line parameters have been obtained from the analysis of room temperature recordings of the spectrum of pure water and recordings of the spectra of heated water/nitrogen mixtures. The recordings of the water vapor spectrum were obtained with Fourier Transform Spectrometers at Kitt Peak and at the Justus-Liebig-Universität Giessen. Up to eighteen spectra have been fitted simultaneously with a multispectrum nonlinear least-squares fitting technique (1) developed by Dr. D. Chris Benner and colleagues.

II. Background

Detailed, precise information about the infrared spectrum of water vapor is vital in the interpretation of satellite data of the Earth's atmosphere. Present information on water vapor line positions, line strengths, line widths and line shifts available in atmospheric databases is useful, but incomplete.

The results presented here complement existing knowledge of line parameters by providing experimentally determined broadening and shifting coefficients for selected transitions. Self-broadening coefficients, for example, have been investigated by Mandin et al (2) in this region in 1982 (and more recently in nearby regions by Toth et al (3)), but are not included in HITRAN96 in this region (around 3500 cm^{-1}). The air broadening coefficients given in HITRAN96 are those converted from calculated values for line widths in nitrogen by Gamache and Davies (4) using the expression

$$b_L{}^\circ(H_2O\text{-air}) = 0.90\ b_L{}^\circ(H_2O\text{-}N_2)$$

In addition, the temperature dependence n of the air broadening coefficient

$$b_L{}^\circ(T) = b_L{}^\circ(T_o)\left(\frac{T_o}{T}\right)^n$$

is fixed at 0.64 in HITRAN96 for all transitions in this region.

This work provides estimates of the temperature dependence n for selected transitions, and provides experimentally determined self- and nitrogen-broadened widths.

The shifting coefficients as a result of increasing pressure of perturbing gas (nitrogen, in this case) have also been determined. The model used for these determinations was

$$d = do + d' \ (T-T_o).$$

III. Experimental Data

Two sets of data were fit simultaneously using LABFIT (1). The first set (heated water vapor in nitrogen) was collected with the McMath Fourier Transform spectrometer in 1994 using a heatable multireflection cell at the National Solar Observatory on Kitt Peak. These data provide information on nitrogen-broadened widths and shifts, and the temperature dependence of these widths and shifts. The second set of data (heated water vapor) was collected in 1998 using a single path temperature controlled absorption cell and the Bruker IFS120 HR located at the Justus-Liebig-Universität- Giessen, Germany. These data provide information on self-broadened widths and the temperature dependence of these widths. The measurement parameters for these recordings are summarized in Tables 1 and 2.

IV. Results of Work

Analysis of the spectra has resulted in improved line parameters for 131 lines in the region to date. The majority of the lines belonged to the v_1 (62) and v_3 (38) bands. The rest of the transitions were from the $2v_2$ (15), $v_2+v_3-v_2$ (12) and $v_2+v_1-v_2$ (4) bands.

Parameters were determined for water vapor perturbed by nitrogen and by water. The error bars in the figures represent two standard deviations. The horizontal axis in many figures provides information on the rotational characteristics of the transition (jm is the maximum j value, km the maximum k value) in the notation used by Toth, Brown and Plymate (3).

Parameters determined pertaining to nitrogen perturbation include nitrogen-broadened widths (Figures 1 and 2), temperature dependence of nitrogen-broadened widths

(Figure 3a), nitrogen-induced line shifts (Figures 4 and 5), and temperature dependence of nitrogen-induced line shifts (Figure 6a and 6b).

Parameters determined pertaining to water perturbation include self-broadened widths (Figures 7 and 8) and temperature dependence of self-broadened widths (Figure 3b).

The results obtained have been compared with selected available values in the literature (2) (Figure 9) and HITRAN (Figure 10). Table 3 provides a comparison of self-broadened line widths determined here with those determined by Mandin and co-workers (2). Error bars have been omitted in Figures 9 and 10. An overview of the comparison between the parameters found by this work and the values available in the HITRAN96 database is found in Figures 11 – 13.

Figure 11 illustrates a comparison of Nitrogen broadened widths of water lines, computed by (This work-HITRAN)/HITRAN. HITRAN values are actually for air-broadened widths, and these were converted to nitrogen-broadened widths for comparison. J" is the J value for the lower state. Note that there are greater differences between values in this work and values from HITRAN for the higher J transitions. Figure 12 provides a comparison of line intensities from this work with those available in HITRAN96. The values plotted here were computed by (This work – HITRAN96)/ HITRAN96. The horizontal axis represents the natural logarithm of the intensity of the line. Note that deviations are much greater for weaker lines, and that intensities found in this work are generally 10-20% higher than HITRAN96 for the strongest, and thus most frequently measured lines. Figure 13 provides a comparison of line positions from this work with those provided in HITRAN96. The values plotted here were computed as (This work – HITRAN96). The line position and line strength information in HITRAN96 is the same as that provided in HITRAN86, when the positions and strengths were updated to include those published by Camy-Peyret, Flaud and Toth in their 1981 water vapor line atlas (5). In cases in which the 1981 line positions are contradicted by more recent works (6,7,8), the line position values are generally off the scale and are not included in Figure 13. Affected transitions, however, were included with their correctly fitted line positions in the fits performed.

The wavenumber calibration of the Giessen data is presently a subject of discussion with the Giessen lab. As soon as these difficulties are resolved the self-shifting

determined for sixty transitions in this region, but are too heavily influenced by the questionable wavenumber calibration of the Giessen data to be considered reliable. The concentration calibration of the air/water spectra is also under discussion, and fits including these will be performed shortly.

V. Presentation of Work

The work performed in connection with NASA Grant NAG-1-2084 has been the subject of two presentations and is currently being prepared for publication. The two presentations were an invited lecture, "Water, Water Everywhere..., but How Much? Application of Molecular Spectroscopy to the Study of Earth's Atmosphere" at Ohio Wesleyan University, Delaware, Ohio, December 1998, and the contributed poster "Water Vapor Line Parameters in the 3500-3650 cm^{-1} Region" (with D. C. Benner, V. Malathy Devi, M. A. H. Smith, and M. Lock), poster D26, 16th International Colloquium on High Resolution Molecular Spectroscopy, Université de Bourgogne, Dijon, France, September 1999.

VI. Acknowledgements

I thank Mary Ann Smith and V. Malathy Devi, who collected the Kitt Peak data with Claude Plymate and Jeremy Wagner, and Michael Lock, who collected the Giessen data. I also thank D. Chris Benner for the opportunity to use his excellent program LABFIT.

VII. References

1. D. Chris Benner, C. P. Rinsland, V. Malathy Devi, M. A. H. Smith, and D. Atkins, *JQSRT* **53**, 705-721 (1995).

2. J.-Y. Mandin, C. Camy-Peyret, and J.-M. Flaud, *Can. J. Phys.* **60**, 94-100 (1982).

3. R. A. Toth, L. R. Brown, and C. Plymate, *JQSRT* **59**, 529-562 (1998).

4. R. R. Gamache and R. W. Davies, *Applied Optics* **22**, 4013-4019 (1983).

5. J.-M. Flaud, C. Camy-Peyret, and R. A. Toth, *Water Vapor Line Parameters from Microwave to Medium Infrared* (Pergamon, London, 1981).

6. R. A. Toth, *JOSAB* **10(9)**, 1526-1544 (1993).

7. R.A. Toth, *JOSAB* **10(11)**, 2006-2029 (1993).

8. S. N. Mikhailenko, Vl. G.Tyuterev, K. A. Keppler, B. P. Winnewisser, M. Winnewisser, G. Mellau, S. Klee, and K. Narahari Rao, *J. Mol. Spectrosc.* **184**, 330-349 (1997).

VIII: Tables 1-3

Table 1: Heated Water Vapor /Nitrogen Measurements, National Solar Observatory, Kitt Peak. Absorption Pathlength: 22.35m (baselength .5588m) Resolution (1/MOPD): 0.0106 cm^{-1}, No. of Scans: 6

Temp. (/C)	Pressure (/Torr)		VMR (P_{H_2O}/P)	P_{H_2O} (/Torr)	Recording
	i	f			
101	249.9	249.8	0.000 65	0.16	470
32	0.034	.034	0.40	0.014	471
51	359.8	368.4	0.000 08	0.029	472
51	250.2	251.2	0.000 1	0.025	473
51	0.590	0.629	0.52	0.31	474
51	400.5	400.4	0.000 7	0.28	475
51	225.7	225.8	0.001 2	0.27	476
100	1.741	2.269	0.93	1.86	477
100	420.9	421.2	0.004	1.69	478
100	208.6	209.1	0.007 8	1.62	479
150	375.2	376.3	0.009 2	3.45	481
150	176.1	177.4	0.02	3.15	482

Table 2: Heated Water Vapor Measurements, Justus-Liebig-Universität Giessen, Germany. For all recordings: Absorption Path length: 3.02m Resolution (1/MOPD): 0.00556 cm^{-1}

Spectrum	Pressure (/mbar)		Temp. (/C)		Scans	Signal-to-Noise (pp/rms)
	i	f	i	f		
C	0.52	0.55	49.75	49.8	600	560/2600
F	1.05	1.08	49.80	49.8	600	720/3130
G	2.65	2.68	99.60	99.7	600	550/2610
H	5.33	5.22	99.70	99.7	323	570/2430
I	5.30	5.34	144.1	144.3	600	171/790
J	10.73	10.85	144.4	144.5	600	280/1240

Table 3: Comparison of Self-Broadened Widths with Ref. (2)

Band	Position /cm^{-1}	J'	Ka'	Kc'	J"	Ka"	Kc"	This Work	% Error	Mandin (2)	% Error	Pred (2)
$2\nu_2$	3520.239	7	2	5	6	1	6	0.470	24	0.485	18	
$2\nu_2$	3506.705	6	4	3	5	3	2	0.410	4	0.452	20	
ν_1	3500.877	9	2	8	9	3	7	0.304	11	0.364	18	
ν_1	3501.226	8	4	5	8	5	4	0.393	4	0.346	18	
ν_1	3511.596	4	1	3	5	2	4	0.412	1	0.61	20	
ν_1	3512.609	7	4	3	7	5	2	0.395	4	0.375	18	
ν_1	3513.835	7	4	4	8	3	5	0.383	2	0.384	17	
ν_1	3514.048	9	1	8	9	2	7	0.348	2	0.374	18	
ν_1	3514.167	5	4	1	5	5	0	0.351	3	0.336	18	
ν_1	3519.850	8	2	7	8	3	6	0.357	2	0.461	20	
ν_1	3521.294	8	3	6	8	4	5	0.311	4	0.42	23	
ν_1	3526.395	9	5	4	10	4	7	0.137	24	0.356	18	
ν_1	3530.073	7	3	5	7	4	4	0.434	2	0.382	20	
ν_1	3530.760	5	1	5	6	0	6	0.348	4	0.578	30	.471
ν_1	3540.175	5	3	3	5	4	2	0.417	2	0.471	23	
ν_3	3501.064	8	5	4	9	5	5	0.340	2	0.341	20	
ν_3	3506.083	5	3	2	5	5	1	0.346	8	0.323	18	
ν_3	3513.072	3	1	3	4	3	2	0.459	8	0.609	20	.471
ν_3	3518.992	4	1	3	5	3	2	0.460	4	0.661	23	.502
ν_3	3521.118	7	2	6	7	4	3	0.444	22	0.496	23	
ν_3	3531.376	7	4	3	8	4	4	0.343	4	0.426	20	
ν_3	3534.272	6	1	6	6	3	3	0.451	4	0.459	17	
ν_3	3538.785	6	2	5	6	4	2	0.310	12	0.562	20	.473

IX: Figures 1-13

Figure 1: Nitrogen-broadened widths in v_1 of H_2O. The horizontal axis describes the rotational characteristics of the transition (jm is the maximum j value, km the maximum k value).
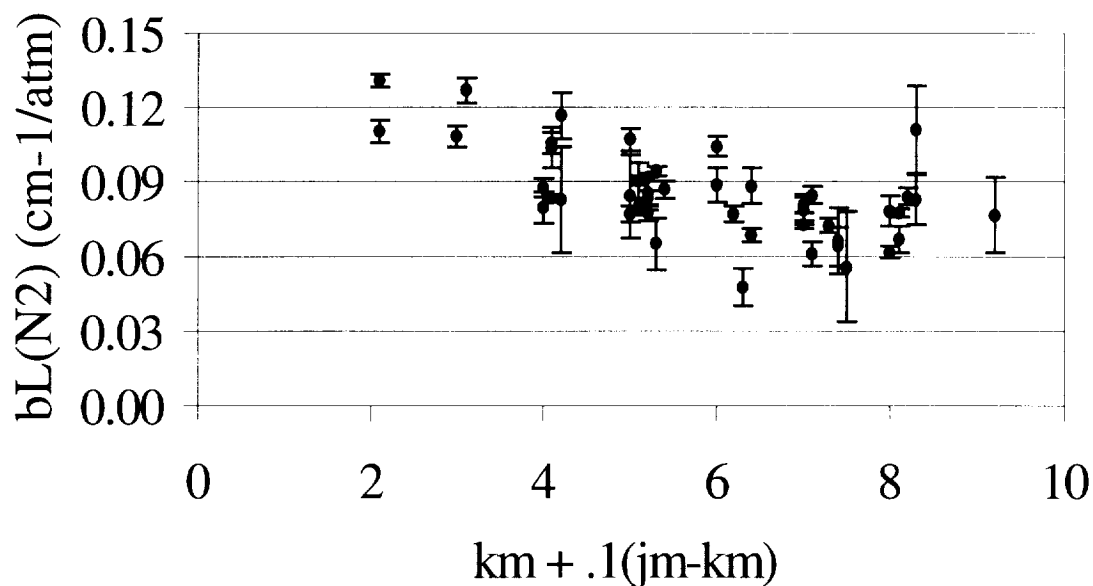

Figure 2: Nitrogen-broadened widths in v_3 of H_2O. The horizontal axis describes the rotational characteristics of the transition (jm is the maximum j value, km the maximum k value).
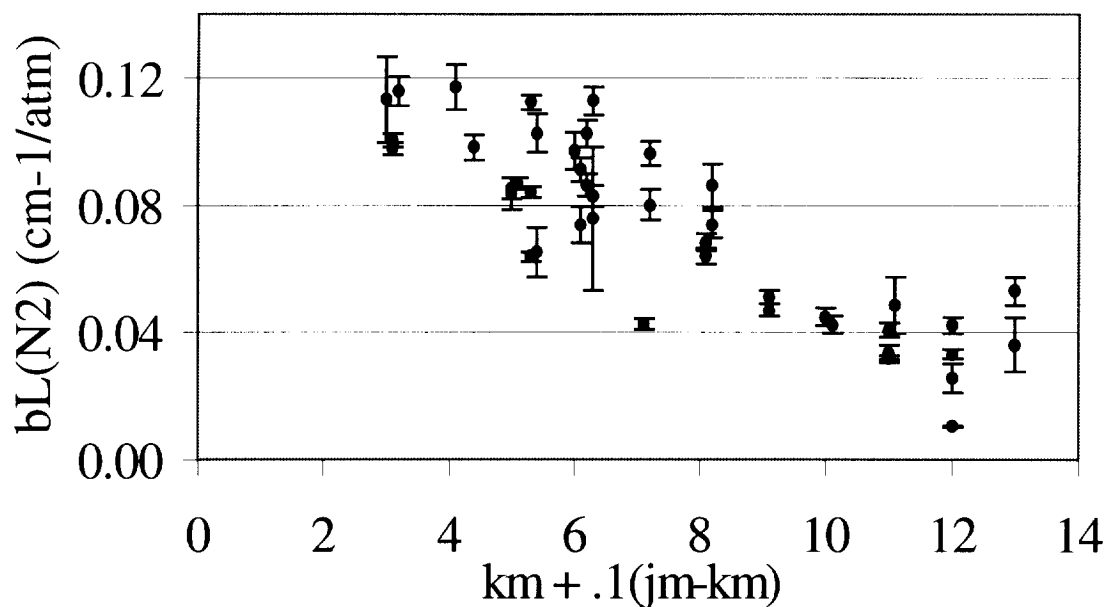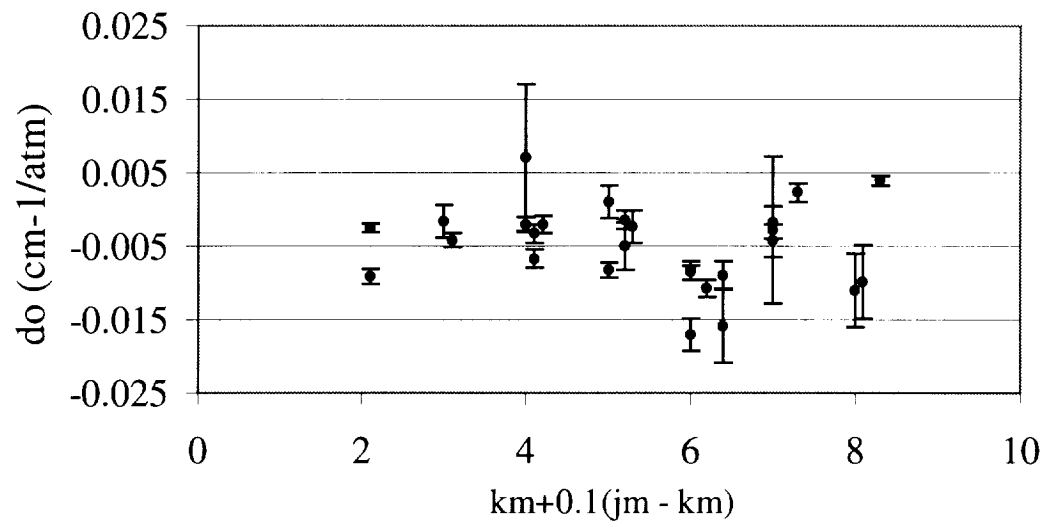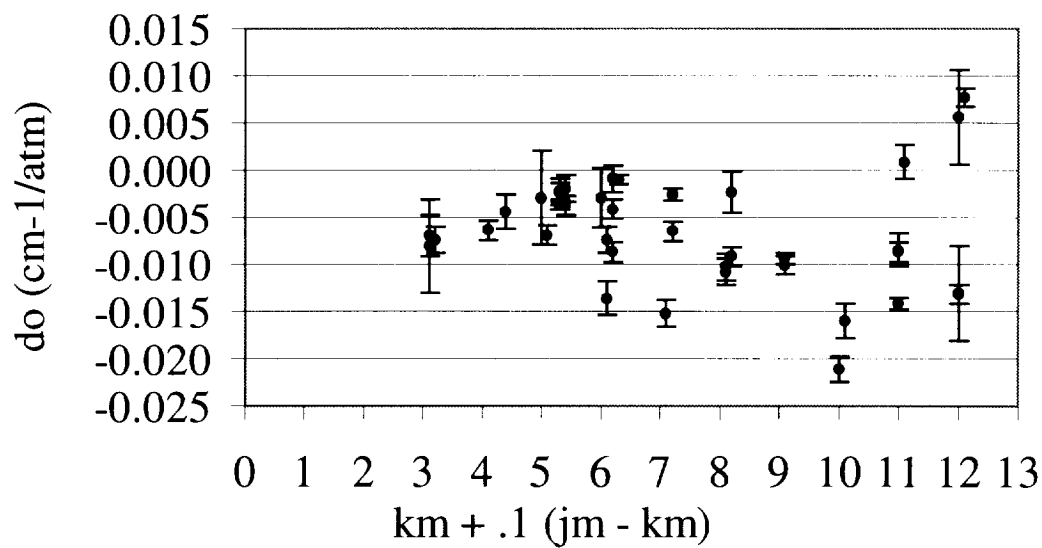
Figure 3: Temperature dependence of perturber-induced Widths: Figure 3a: Perturber: N_2: v_1 lines are represented by the triangles and have slightly higher n values than the v_3 lines, which are represented by squares. These values are compared to the standard value for HITRAN which is 0.64 (dashed line). The horizontal axis describes the rotational characteristics of the transition: jm represents the maximum j number, and km represents the maximum k number.
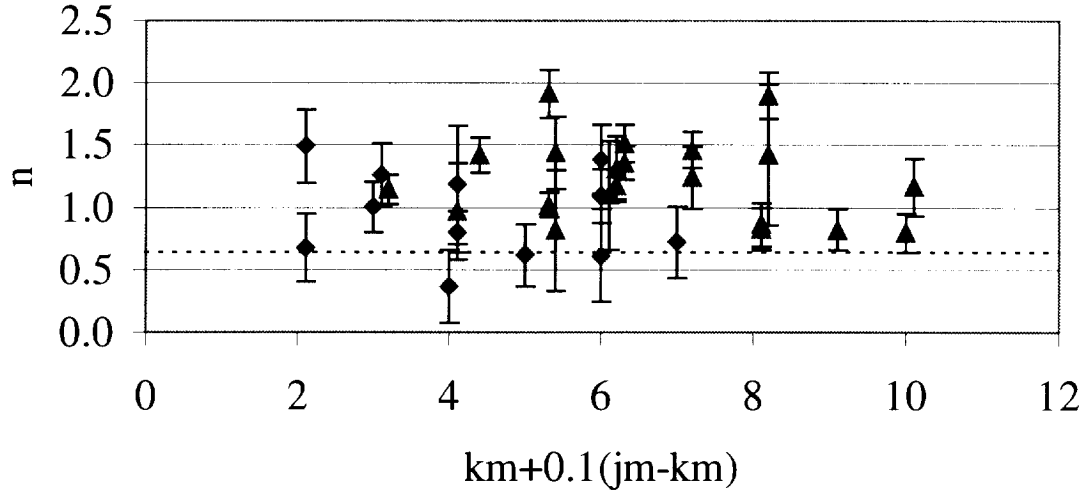
Figure 3b: Perturber: H_2O: v_1 lines are represented by the triangles and have slightly higher n values than the v_3 lines, which are represented by squares. These values are compared to the standard value for HITRAN which is 0.64 (dashed line). The horizontal axis describes the rotational characteristics of the transition: jm represents the maximum j number, and km represents the maximum k number.
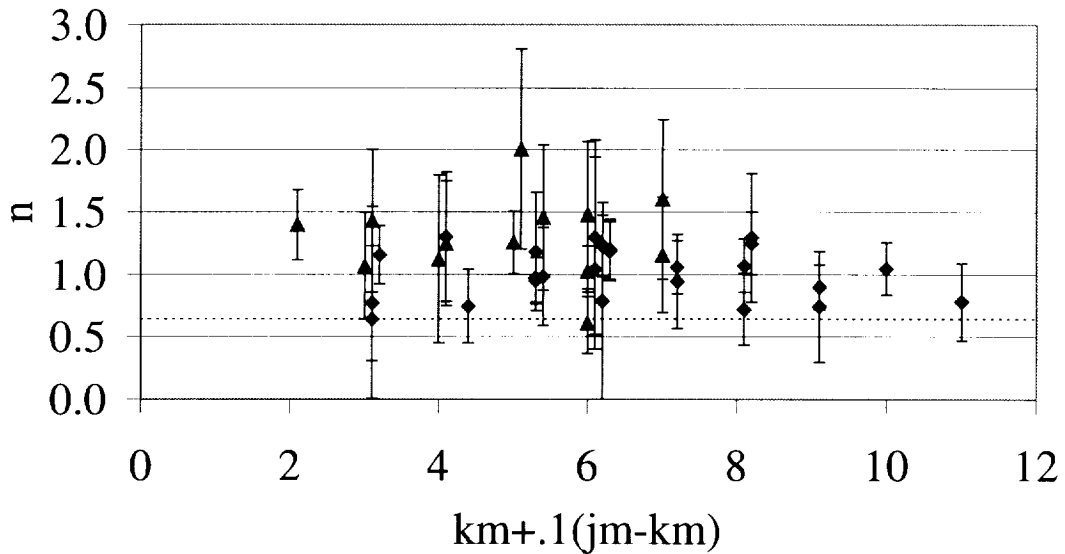
Figure 4: Nitrogen-pressure-induced line shifts in v_1 of H_2O. The horizontal axis describes the rotational characteristics of the transition (jm is the maximum j value, km the maximum k value).

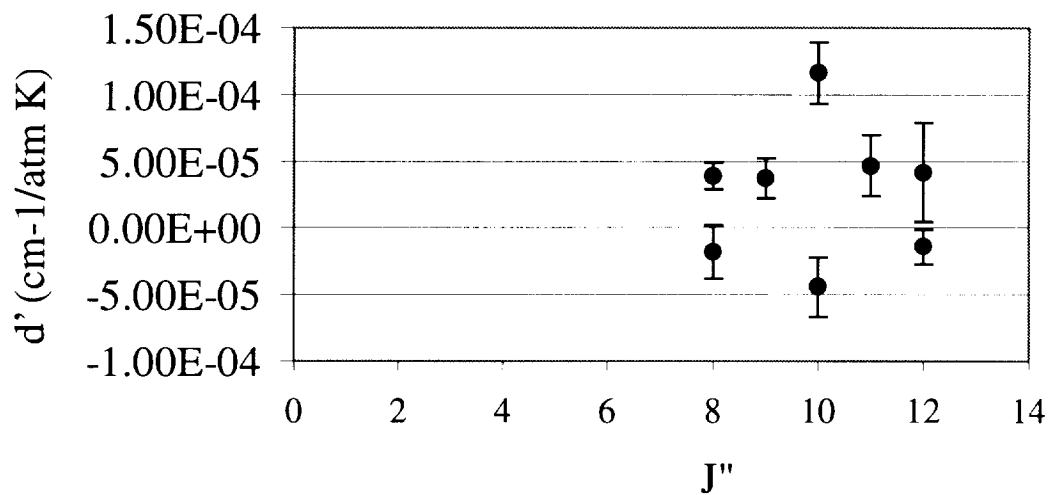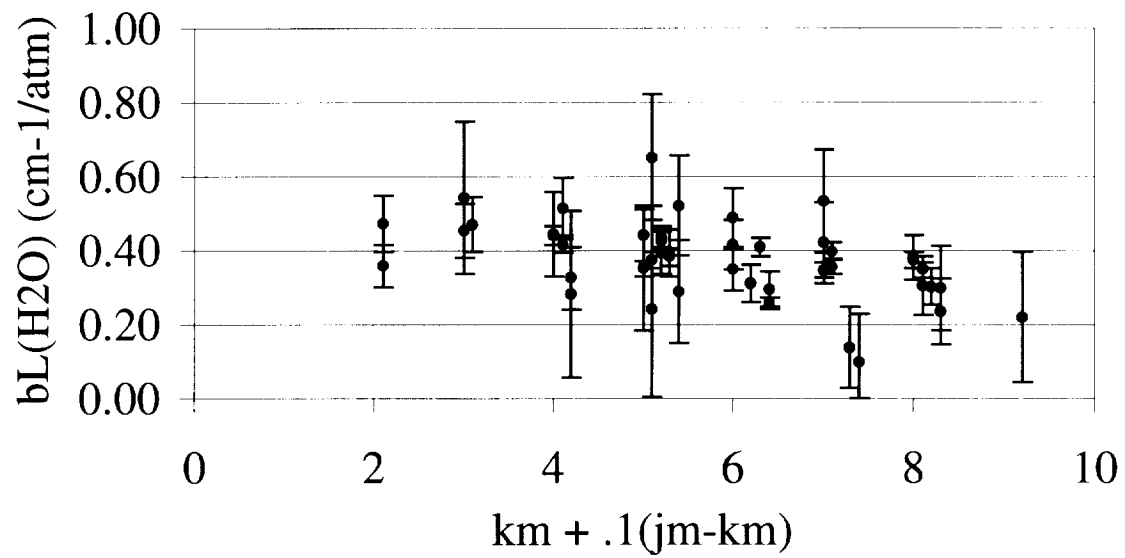Figure 5: Nitrogen-pressure-induced line shifts in v_3 of H_2O. The horizontal axis describes the rotational characteristics of the transition (jm is the maximum j value, km the maximum k value).

Figure 6a: Temperature dependence of nitrogen-pressure-induced line shifts in v_1 of H_2O. J" is the lower state J value.
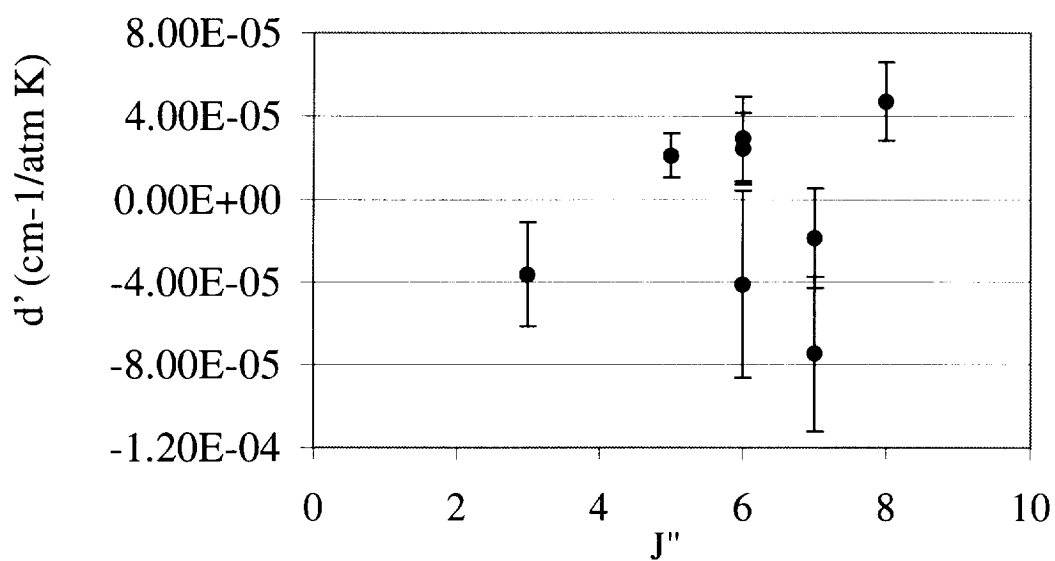
Figure 6b: Temperature dependence of nitrogen-pressure-induced line shifts in v_3 of H_2O. J" is the lower state J value.

Figure 7: Self-broadened widths in v_1 of H_2O. The horizontal axis describes the rotational characteristics of the transition (jm is the maximum j value, km the maximum k value).

Figure 8: Self-broadened widths in v_3 of H_2O. The horizontal axis describes the rotational characteristics of the transition (jm is the maximum j value, km the maximum k value).
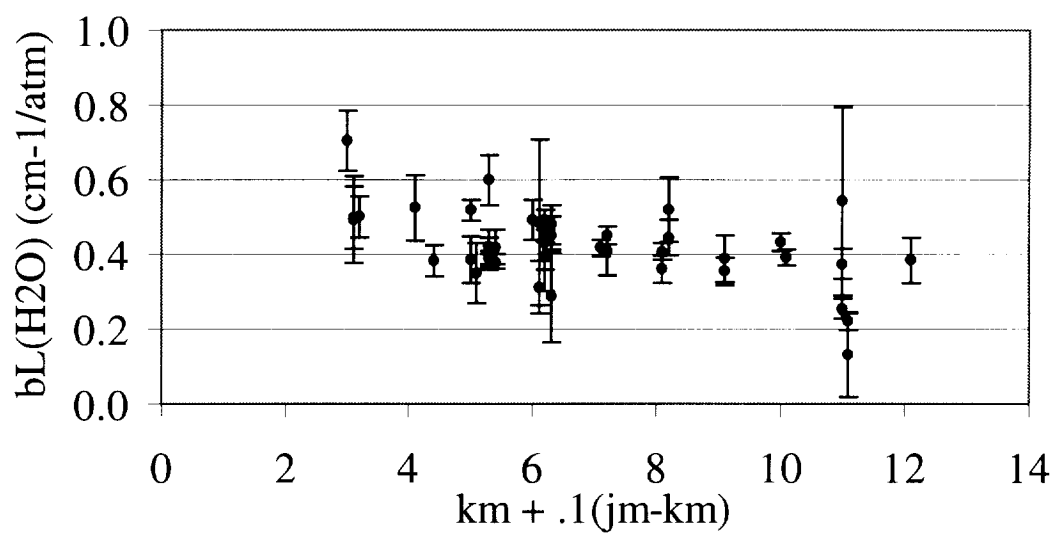
Figure 9: Comparison of results of this work with results of the work of Mandin et al (2). The values obtained from this work appear on the x axis and the values from Ref. 2 appear on the y axis. The asterisks denote calculated values from Ref. 2 for several lines for which Mandin et al had large uncertainty in experimentally determined values.
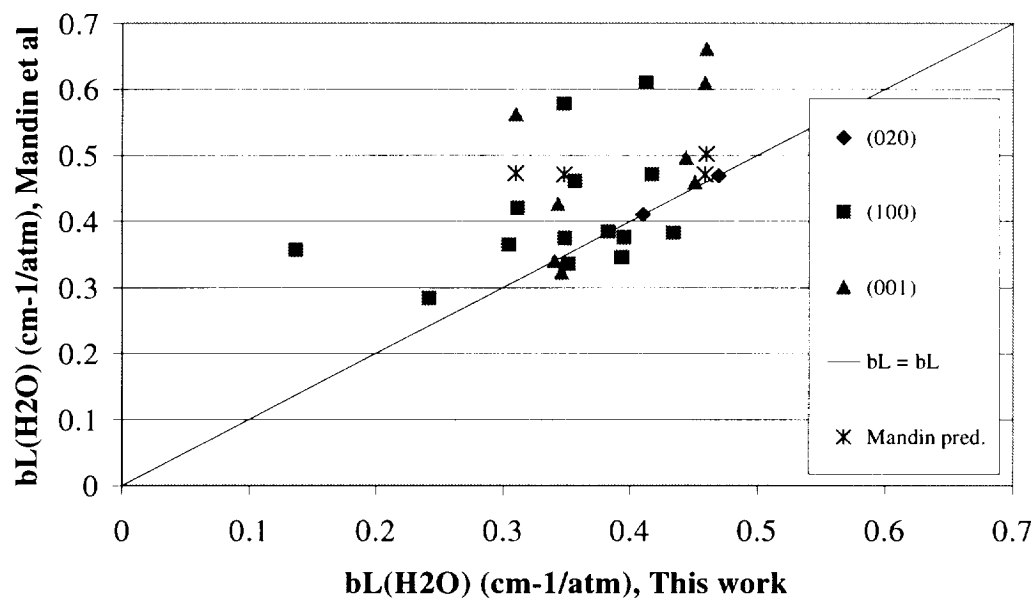

Figure 10: Comparison of results of this work with values from HITRAN96. The values obtained from this work appear on the x axis and the values from HITRAN on the y axis.
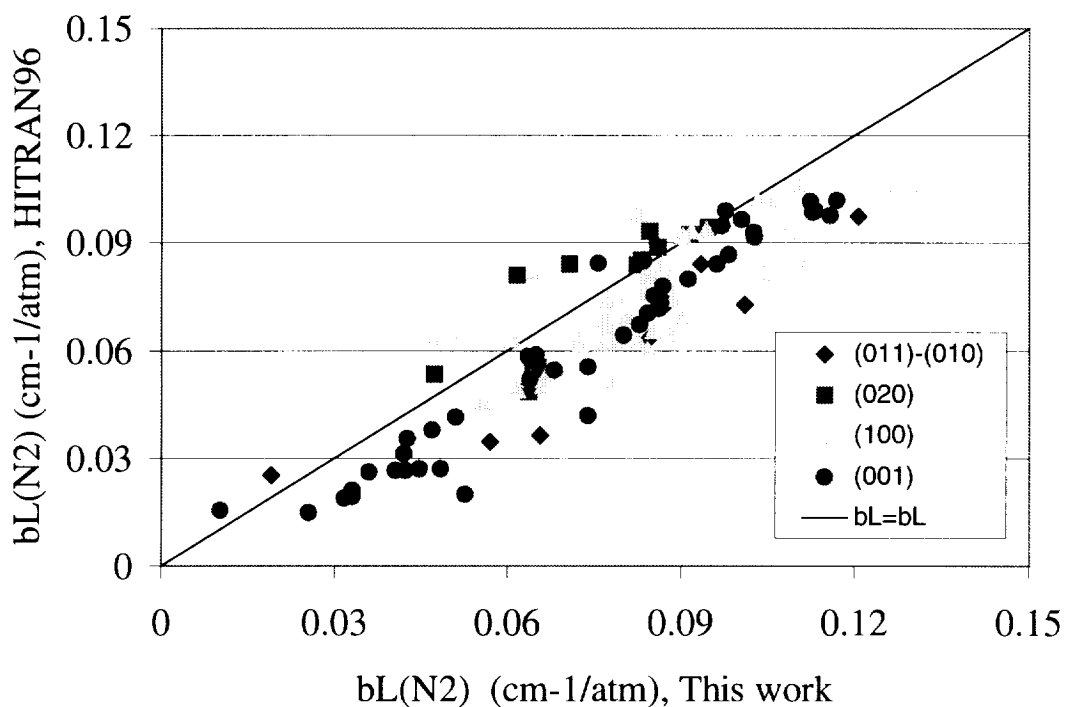
Figure 11: Comparison of Nitrogen broadened widths of water lines, computed by (This work-HITRAN)/HITRAN. HITRAN values are actually for air-broadened widths, and these were converted to nitrogen-broadened widths for comparison. J" is the J value for the lower state.
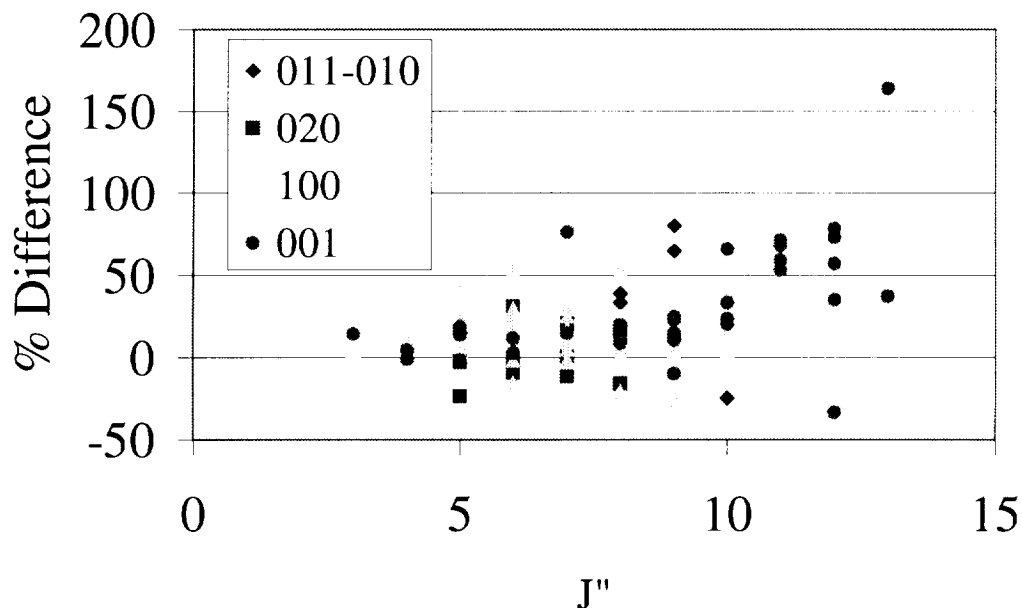

Figure 12: Comparison of line intensities from this work with those provided in HITRAN96. The values plotted here were computed as (This work – HITRAN96)/ HITRAN96. The horizontal axis represents the natural logarithm of the intensity of the line. Note that deviations are much greater for weaker lines, and that intensities found in this work are generally 10-20% higher than HITRAN96 for the strongest lines.
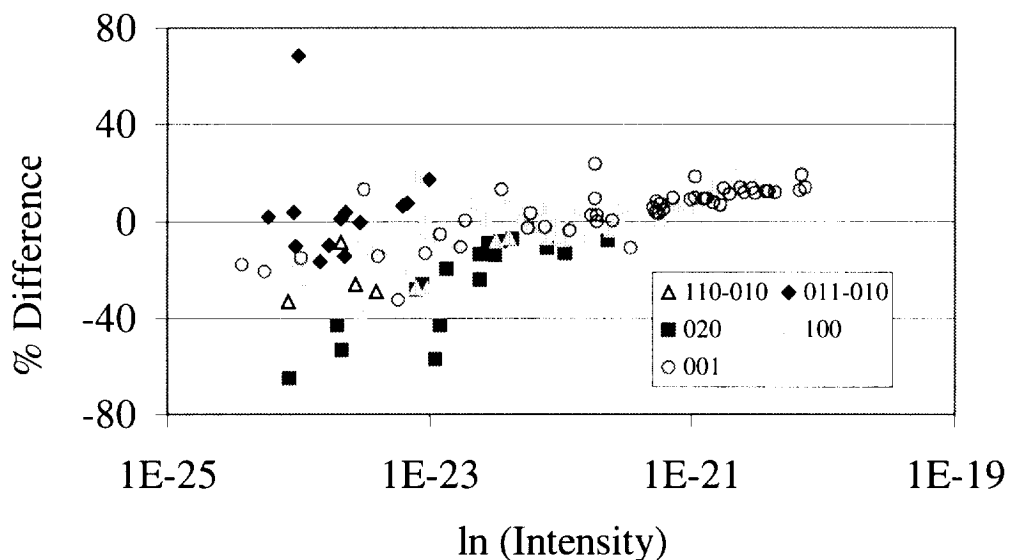
Figure 13: Comparison of line positions from this work with those provided in HITRAN96. The values plotted here were computed as (This work – HITRAN96). The horizontal axis represents the rotational characteristics of the transition: jm represents the maximum j number, and km represents the maximum k number.

km + 0.1(jm-km)